Repurposing an orally available drug for the treatment of geographic atrophy

Chulbul M. Ahmed, Manas R. Biswal, Hong Li, Pingyang Han, Cristhian J. Ildefonso, Alfred S. Lewin

Department of Molecular Genetics and Microbiology, University of Florida, Gainesville, FL

Purpose: Chronic oxidative stress and subacute inflammation have been implicated as causes of age-related macular degeneration (AMD). In this study, we tested whether an orally available 5-OH-tryptamine (5HT) 1a receptor agonist, xaliproden, could protect against retinal pigment epithelium (RPE) cell damage in culture and in a mouse model of geographic atrophy.
Methods: Paraquat was used to create mitochondrial oxidative stress in ARPE-19 cells, and tumor necrosis factor-α (TNF-α) was used to stimulate the production of inflammatory cytokines in these cells. The production of antioxidant proteins, metallothionein, and inflammatory cytokines was assayed with quantitative real-time PCR. Cell survival was analyzed with microscopy and a cell titer assay. Integrity of the RPE monolayer was determined by measuring the transepithelial electrical resistance (TEER) and with immunocytochemistry with zona occludens protein 1 (ZO-1) antibody. RPE atrophy was studied in mice deleted for *Sod2* (the gene for mitochondrial superoxide dismutase) specifically in the RPE. The mice were treated orally with daily doses of xaliproden at 0.5 and 3 mg/kg for 4 months. The retinal structure was analyzed with spectral domain optical coherence tomography (SD-OCT) and with light and electron microscopy. Retinal function was assessed with full-field electroretinography (ERG) and with optokinetic measurements.
Results: Xaliproden led to a dose-dependent increase in cell survival following treatment with paraquat. Synthesis of the antioxidant response genes *NqO1*, *GSTM1*, *CAT*, *HO-1*, and *Nrf2* was increased in response to the drug, as was the zinc chaperone metallothionein. Treatment of cells with TNF-α led to increased production of IL-1β, IL-6, chemokine (C-C motif) ligand 20 (CCL20), and vascular endothelial growth factor (VEGF) by ARPE-19 cells, and this response was attenuated by treatment with xaliproden. TNF-α also led to a decrease in the TEER that was prevented by treatment with the 5HT1a agonist. Daily gavage with xaliproden at either dose induced the production of protective enzymes in the mouse retina, and treatment of the *Sod2*-deleted mice with the drug showed improved thickness of the outer nuclear layer and improved visual acuity relative to the control-treated mice. There was no significant difference in full-field scotopic ERG among the treatment groups, however. Vacuolization of the RPE and disorganization of the photoreceptor outer segments were reduced at both dose levels of xaliproden.
Conclusions: Xaliproden protected RPE cells from oxidative and inflammatory insults and protected the mouse RPE and retina from RPE atrophy in the face of excess mitochondrial oxidative stress. These results suggest that this drug, which had a reasonable safety profile in clinical trials, may be used to prevent the progression of geographic atrophy in humans.

The 5H1a receptor is a seven-membrane spanning domain G-protein-coupled receptor that is expressed in many cell types [1]. Agonists of this receptor are currently in clinical use for treatment of anxiety, and such drugs have exhibited neuroprotective properties in spinal cord injury [2], Parkinson disease models [3,4], and excitotoxicity [5]. In the eye, Collier and colleagues demonstrated that two different 5HT1a agonists provided nearly complete protection against phototoxic injury in albino rats when given systemically before and shortly after exposure to bright light [6]. In a subsequent paper, the same group demonstrated that one of these compounds (AL-8309A) blocked the deposition of complement related proteins and the activation of microglial following severe photo-oxidative stress [7].

In earlier work, we showed that a prototype 5HT1a agonist, 8-hydroxy-2-dipropylaminotetralin (8-OH-DPAT), protected ARPE-19 cells from oxidative damage by hydrogen peroxide and by paraquat, and that daily administration of 8-OH-DPAT to mice prevented injury to the RPE and neural retina in two mouse models of geographic atrophy caused by depletion of manganese superoxide dismutase (MnSOD) in the RPE [8,9]. Those experiments required daily injections of the compound, which is not approved for human use. We wanted to determine whether a similar effect could be achieved using a drug that has been tested in patients and is available orally.

Xaliproden is a highly selective synthetic 5HT1a receptor agonist [10]. It crosses the blood–brain barrier and can be taken by mouth. The drug increases the release of dopamine

Correspondence to: Alfred S. Lewin, Department of Molecular Genetics and Microbiology, University of Florida, 1200 Newell Dr., Gainesville, FL, 32610-0266; Phone: (352) 392-0676; FAX: (352) 273-8905; email: lewin@ufl.edu

in the prefrontal cortex of rats and decreases the level of extracellular serotonin in the ventral hippocampus. Both effects are attributable to binding of the 5HT1a receptor and can be inhibited by pretreatment with a 5HT1a antagonist, WAY100635 [11]. The activity of xaliproden appears to be mediated by the mitogen-activated kinases Erk1 and Erk2 [12]. Xaliproden also has neurotrophic properties that are dependent on binding to the 5HT1a receptor. This drug has been tested in humans as a potential treatment for amyotrophic lateral sclerosis (ALS) [13] and Alzheimer disease (Clinicaltrials.gov NCT00103649). Although no efficacy was demonstrated in these studies, the drug appears to relieve allodynia associated with chemotherapeutic agents such as paclitaxel [14], and xaliproden has been tested for this indication in cancer patients (Clinicaltrials.gov NCT00272051).

Because of the protective effect of 8-OH-DPAT in our mouse model of retinal degeneration, we wanted to test xaliproden in the same model, particularly since the drug's safety profile and side effects have been established in several clinical trials. We began by testing the compound on an RPE-derived cell line to determine the impact on the expression of antioxidant genes and on proinflammatory cytokines. We then determined that orally administered xaliproden preserved visual function and RPE structure in mice subjected to chronic mitochondrial oxidative stress.

METHODS

Cell culture and RNA analysis: We obtained validated ARPE-19 cells (CRL-2301, Appendix 1) from the American Type Culture Collection (Manassas, VA) and froze cells from the first culture immediately. We discarded the ARPE-19 cells after three subsequent passages. To extract RNA, cells were grown to 90% confluence and then placed in a 1:1 mixture of Dulbecco's Modified Eagle Medium (Sigma-Aldrich, St. Louis, MO) and Ham's F12 nutrient mixture (DMEM/F12) plus 1% fetal bovine serum (FBS). We treated the cells with 20 µM xaliproden (R&D Systems, Minneapolis, MN) plus or minus 20 ng/ml TNF-α (PeproTech, Rocky Hill, NJ) or 300 µM paraquat (Sigma-Aldrich, St. Louis, MO) for 24 h. We washed the cells with PBS (120 mM NaCl, 20 mM KCl, 10 mM $NaPO_4$, 5 mM KPO_4, pH 7.4), pH 7.4 and extracted RNA using the RNeasy Mini Kit (Qiagen, Valencia, CA). We then synthesized cDNA using the iScript cDNA synthesis kit (Bio-Rad, Hercules, CA) and amplified PCR products (The PCR reaction mixture contained 3 µM gene specific primers. After denaturation at 95 °C for 2 min, 40 cycles of amplification (94 °C for 15 seconds; 60 °C for 30 seconds).) using the gene-specific primers listed in (Appendix 2) and the SsoFast EvaGreen Supermix (Bio-Rad). We amplified β-actin

cDNA from each sample to serve as an internal standard. We used the system software from the CFX96 real-time thermal cycler (Bio-Rad) to compare transcript levels in the treated and untreated samples.

Immunohistochemistry of cultured cells: We grew ARPE-19 cells in DMEM/F12 plus 1% FBS for 4 weeks in eight-well chambered slides. By this time, the cells had assumed a cobblestone appearance characteristic of the RPE. We then subjected them to treatment with 300 µM paraquat, 20 µM xaliproden, or both for 48 h. We fixed the cells using freshly prepared 4% paraformaldehyde for 30 min and washed them once with PBS. Cells were made permeable by treatment with 1% Triton X-100 in PBS for 30 min. We exposed the cells to 10% normal goat serum in PBS plus 0.5% Triton X-100 for 30 min to reduce background antibody binding. We then washed the cells in 0.2% Triton X-100 in PBS and then incubated them in the same buffer with a 1:200 dilution of polyclonal antibody to ZO-1 (Invitrogen, Grand Island, NY) for 15 h at 4 °C. They were washed in PBS + 1% Triton X-100 three times and then incubated with secondary antibody (Cy-3 conjugated goat anti rabbit; Invitrogen) for 30 min at room temperature followed by three additional wash steps. After they were covered with a coverslip, we imaged the cells in a fluorescence microscope.

ELISA: IL-1β secreted from ARPE-19 cells was assayed using an enzyme-linked immunosorbent assay (ELISA) kit (BioLegend, San Diego, CA) following the manufacturer's protocol. Briefly, we coated microtiter plates with capture antibody by incubation overnight at 4 °C. The wells were washed and then incubated with a blocking buffer for 2 h at room temperature, followed by three washings. We added different dilutions of the supernatants from ARPE-19 cells to the wells in triplicate and incubated the cells for 2 h, followed by three washings with the wash buffer. We then added detection antibody and incubated the cells for 1 h, followed by three washings. Avidin-horseradish peroxidase (HRP) was added for 0.5 h, followed by three washes. Substrate was added for 0.5 h, and the reaction was stopped with the stop buffer. The absorbance was measured in a microplate reader at 450 nm.

Measurement of transepithelial electrical resistance: We plated the ARPE-19 cells on Transwell inserts (33.6 mm², pore size 0.4 µm; Greiner Bio-One, Monroe, NC) in DMEM/F12 including 1% FBS and allowed the cells to grow in 24-well plates for 4 weeks. We added paraquat plus or minus xaliproden at the concentrations used above, and the cells were incubated for an additional 48 h. We used an EVOM2 volt/ohm meter (World Precision Instruments, Sarasota, FL) to measure the transepithelial electrical resistance (TEER) at room temperature as specified by the manufacturer.

We calculated the net resistance values by subtracting the measurement of a blank well from the measurements of the wells that contained cell monolayers.

Drug delivery in a mouse model of geographic atrophy: We conducted all animal procedures in accordance with the Association for Research in Vision and Ophthalmology (ARVO) Statement for the Use of Animals in Ophthalmic and Vision Research. The University of Florida Institutional Animal Care and Use Committee reviewed and approved all animal procedures in advance. Details of the mouse model are provided in our earlier publication [15]. Depletion of manganese superoxide dismutase either by ribozyme knockdown or by deletion of Sod2 in the RPE (retinal pigment epithelium) of mice leads to characteristic features of dry AMD including disruption of Bruch's membrane, increased accumulation of bisretinoid compounds, increase in RPE lipofuscin and CEP-modified proteins, localized death of RPE cells and overlaying photoreceptors [8,15-17]. For the current experiments we employed mice with a specific deletion of Sod2 in the RPE [9,15]. Briefly, we employed C57Bl/6J mice transgenic for P_{VMD2}-*rtTA* and *tetO-P*$_{hCMV}$*cre* [18] and homozygous for a "floxed" (flanked by *loxP*) of *Sod2*, the gene for MnSOD [19]. We induced the expression of cre recombinase by feeding doxycycline containing chow (200 mg/kg in Harlan Rodent Diet 7012, Harlan Teklad, Indianapolis, IN) to nursing dams for 2 weeks after delivery. We refer to these animals as *Sod2*$^{loxP/loxP}$ *RPE-cre* mice. Of note, the first time point of ERG analysis was 2 weeks after the cessation of doxycycline, and by 1 month of age, cre recombinase is not detectable in the RPE.

Cohorts of 24 *Sod2*$^{loxP/loxP}$ *RPE-cre* mice received a daily dose of xaliproden by gavage at 0.5 mg/kg or 3 mg/kg of drug dissolved in 0.3% carboxymethylcellulose plus 0.25% Tween-20 (vehicle). An additional cohort of mice was treated with vehicle only. Sub-groups of 14 mice randomly selected were analyzed at monthly intervals with full-field scotopic electroretinography (ERG) and spectral domain optical coherence tomography (SD-OCT) with methods described in the paper by Mao et al. [15]

Optokinetic measurements: In eight randomly selected mice from each treatment group, we measured the visual acuities of treated and untreated eyes by observing the optokinetic responses of mice to rotating sinusoidal gratings (Opto-Motry™) [20]. This method measures the acuities of the left and right eyes independently based on their sensitivities to rotating patterns of bars: Right eyes are more sensitive to counterclockwise rotation, and left eyes are more sensitive to clockwise rotation. The methods we used to measure acuity are described by Pang et al. [21]. Briefly, an unrestrained

mouse was placed on a pedestal located in the center of four LCD computer monitor screens and was observed by an overhead video camera. A trial was initiated by presenting the mouse with the sinusoidal pattern rotating either clockwise or counterclockwise as determined randomly by the system software. Initially, the 100% contrast pattern had a spatial frequency of 0.200 cycles/degree for both directions of rotation. We determined the thresholds for each eye simultaneously using incremental functions for correct responses in both directions. We defined acuity as the highest spatial frequency yielding a threshold response at 100% contrast.

Electroretinography: We performed full-field electroretinography as described in our earlier study on 8-OH-DPAT [9]. After overnight dark adaptation and ketamine/xylazine anesthesia (95 mg/kg ketamine and 5 mg/kg xylazine in 100 µl given i.p.), we recorded responses from both eyes using an LKC UTAS Visual Electrodiagnostic System with a BigShot™ full-field dome (LKC, Gaithersburg, MD). Scotopic ERGs were elicited with 1 msec flashes of white light at 0 dB (2.68 cds/m^2), −10 dB (0.18 cds/m^2), and −20 dB (0.02 cds/m^2). Ten scans were averaged at each light intensity. We then exposed mice to a 2 min white light bleach in the Ganzfeld dome and then to a white flash at 1.0 cd sec/m^2 intensity to elicit a cone response. The a-wave amplitudes were measured from the baseline to the peak in the cornea-negative direction, and the b-wave amplitudes were measured from the cornea-negative peak to the major cornea-positive peak.

Histology and immunohistochemistry of mouse tissue: Mice were injected with 150 mg/kg of sodium pentobarbital (Euthasol) and then perfused with PBS containing 2% paraformaldehyde and 2.5% glutaraldehyde. Mice were enucleated, and the eyes were soaked overnight in 4% paraformaldehyde and 2% glutaraldehyde. We soaked the tissue in 0.1 M cacodylate buffer (pH7.4) for 10 min and incubated it in 1% osmium tetroxide for 4 h at 4 °C in the same buffer. We then soaked the tissue overnight in cacodylate buffer at 4 °C. Subsequently, we dehydrated the tissue in a series of ethanol baths and steeped the tissue in epoxy/propylene on a rotator for embedding. For light microscopy, we prepared 1 µm sections, while for electron microscopy, we prepared sections of 80–100 nm.

For immunohistochemistry, we euthanized mice with inhalation of carbon dioxide. For analysis of retinal sections, eyes were fixed in melting isopentane as described by Wolfrum [22]. We placed cryosections on polylysine-coated slides and soaked them in PBS containing 0.01% Tween-20 for 30 min. We then soaked them in a blocking solution containing mouse immunoglobulin (IgG; Vector® M.O.M.™

Immuno detection kit, cat no. BMK-2202, Burlingame, CA) for 1 h followed by an overnight incubation at 4 °C with primary antibody against carboxyethylpyrrole (CEP) [23] at a dilution of 1:400 in PBS/Tween-20. We washed the sections in the same buffer three times and incubated them for 1 h at room temperature with fluorescently tagged secondary antibody (Alexa Fluor® 594 goat anti-mouse IgG from Life Technologies, Cat No: A11005) plus 4',6-diamidino-2-phenyl-indole (DAPI) to stain the nuclei. We prepared digital micrographs using a Keyence (Itsaca, IL) fluorescence microscope.

Analysis of RNA from tissue: We treated 2-month-old mice with 3 mg/kg of xaliproden by mouth for 4 days. The mice were euthanized with CO_2 inhalation, and RNA was extracted from the dissected retinas using the RNeasy Mini Kit from Qiagen. We performed the cDNA synthesis and qPCR as described for cultured ARPE-19 cells.

Statistical methods: To compare the mean values of several groups (e.g., ERG amplitudes over time), we employed ANOVA with the Newman-Keuls test for multiple comparisons. Except for ERG results, error bars represent the standard deviation. For ERG results, error bars indicate standard error of the mean. We took a significance level $p < 0.05$ as significant. For comparison of RNA levels in treated and untreated cells or mice, we used the Student *t* test for unpaired samples.

RESULTS

Xaliproden protects RPE-derived cells from oxidative injury: Paraquat is an herbicide structurally similar to MPP+, which is known to induce Parkinsonism in animals and humans. Complex III of the mitochondrial electron transport chain (coenzyme Q-cytochrome *c* oxidoreductase) converts paraquat into a free radical that interacts with molecular oxygen to form superoxide [24]. To model mitochondrial oxidative stress in the RPE, we exposed ARPE-19 cells, which are derived from human RPE cells, to paraquat in the presence or absence of 20 µM xaliproden. There is strong pharmacological evidence of 5HT1a receptors on human RPE cells [25]. To determine whether the drug induced the expression of antioxidant genes, we extracted RNA after 15 h, and measured gene expression with quantitative RT–PCR (Table 1).The values in this table represent the RNA levels compared to untreated cells; a value of 1 indicates no change compared to the control. As previously observed using 8-OH-DPAT, we detected a significant induction of genes regulated by the antioxidant response element (NqO-1, GSTM1, HO-1) in response to paraquat or to paraquat plus xaliproden. The induction of *NqO-1* and *GSTM1* was much greater when cells were treated with both compounds, but xaliproden alone did not lead to increased expression of *HO-1* and catalase *(CAT)*.

Interestingly, expression of the transcription factor Nrf2, which regulates these genes, was suppressed by either paraquat or xaliproden but was induced by the combination treatment relative to treatment with paraquat alone. Others have reported that paraquat treatment reduces the levels of Nrf2 in kidney and neuroblastoma cell lines [26,27]; nevertheless, we do not know the cause of the decreased expression of Nrf2 in ARPE-19 cells after paraquat or xaliproden treatment alone. The level of Nrf2 protein is regulated post-transcriptionally, but the promoter of the *Nrf2* gene contains active antioxidant response elements (ARE) suggesting autoregulation of this gene [28]. We also observed a substantial induction in the transcription of metallothionein 1 (a zinc chaperone protein) in the presence of paraquat (5.5-fold) or xaliproden (3.3-fold) and a 10-fold increase in expression by the combination treatment.

To determine whether upregulation of these protective genes correlated with increased cell survival, we measured cell viability in response to paraquat at different concentrations of xaliproden added simultaneously. At 300 µM, paraquat killed more than 80% of the cells after a 24 h incubation, but addition of xaliproden led to an increase in cell viability at all levels tested (Figure 1 and Appendix 3). In our earlier work, we observed a maximum of 60% protection from paraquat-induced oxidative stress with 8-OH-DPAT [9], while up to 80% protection was observed with xaliproden under the same conditions.

ARPE-19 cells form tight junctions similar to RPE monolayers when grown in culture for several weeks in low serum medium. We grew such cells on permeable Transwells and measured the cells' TEER after treatment with paraquat in the presence or absence of xaliproden. Treatment with paraquat caused a greater than 50% drop in the resistance of confluent ARPE-19 cells that had been maintained 4 weeks in 1% FBS medium (Figure 2). Simultaneous treatment with paraquat and xaliproden resulted in no decrease in transepithelial resistance, indicating that the integrity of the monolayer had been maintained. Light micrographs of the ARPE-19 monolayers decorated with primary antibodies to ZO-1 confirmed that elevation of oxidative stress by paraquat disturbed the tight junctions, but they were preserved by simultaneous treatment with xaliproden (Figure 3).

Xaliproden reduces the release of proinflammatory cytokines and the disruption of barrier properties: TNF-α is increased in several retinal diseases involving chronic inflammation, including age-related macular degeneration (AMD) [29]. This cytokine promotes migration and adhesion of RPE cells grown in culture [30], and TNF-α induces the expression of IL-1β, IL-6, and vascular endothelial growth
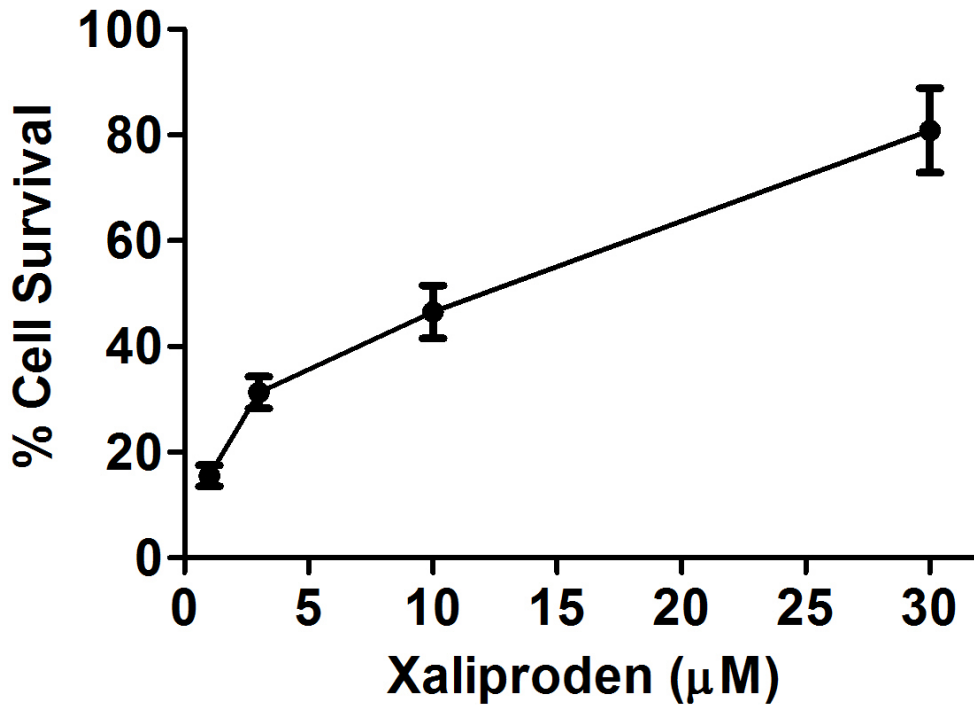
Figure 1. Xaliproden protects ARPE-19 cells against mitochondrial oxidative stress. ARPE-19 cells were seeded in a microtiter plate at 70% confluency and allowed to grow overnight. They were then placed in a serum-free medium and treated with 300 μM paraquat. Increasing amounts of xaliproden were added as indicated, and the cells were incubated for 24 h. Cells were stained with Cell Titer Aqueous (Promega), and the absorbance read in a plate reader. Cell survival was calculated using the absorbance of cells with serum-free media as 100%.

factor (VEGF)-A by RPE cells [31]. To determine whether xaliproden could modulate the expression of cytokines or chemokines induced by TNF-α, we treated ARPE-19 cells with TNF-α in the presence and absence of xaliproden. As expected, treatment of cells with TNF-α alone caused a massive increase in the production of mRNA for IL-1β (171-fold), IL-6 (10.3-fold), and the chemokine CCL-20 (119-fold) relative to untreated cells (Table 2). Treatment of the ARPE-19 cells with xaliproden reduced the impact of TNF-α on the production of inflammatory cytokines. In addition, TNF-α led to a 2.5-fold increase in the synthesis of VEGF-A mRNA, and this effect was abrogated by cotreatment with xaliproden. Members of the IL-6 family protect photoreceptors from light injury and retinal ganglion cells following injury to the optic nerve [32,33], but IL-6 is a proinflammatory cytokine that abrogates immune privilege of the eye [34].

TABLE 1. ENHANCEMENT OF ANTIOXIDANT RESPONSE BY XALIPRODEN.

Target gene	Relative expression ± SD.			P value
	PQ	Xaliproden	PQ +Xaliproden	
NqO-1	2.88±0.35	1.63±0.20	5.76±1.24	0.0014
GSTM-1	1.47±0.02	1.28±0.18	3.24±0.41	0.0002
Nrf 2	0.39±0.01	0.42±0.04	1.94±0.16	<0.0001
Met-1	5.57±0.85	3.34±0.67	9.98±0.75	0.0001
HO-1	2.55±0.25	1.07±0.07	2.48±0.45	0.0016
CAT	1.22±0.07	0.95±0.36	1.82±0.16	0.0095

ARPE-19 cells were seeded at 90% confluency and grown overnight. They were changed into serum free media and treated with 20 μM xaliproden, 300 μM paraquat (PQ), or a combination of two and grown for 24 h. RNA was extracted from these cells and used for cDNA synthesis followed by qPCR with primers for target genes indicated. Assays were performed in three biologic replicates. Values represent average fold change compared to the untreated samples ± s.d. Abbrev: NqO-1, NAD(P)H dehydrogenase quinone 1; GSTM-1, Glutathione ;Met-1, metallothionein-1, HO-1, heme oxygenase 1; CAT, catalase. P values were determined by one-way ANOVA comparing untreated cells and the three treatment groups. To determine the significance, mean values of these groups were compared by ANOVA with the Newman-Keuls *post hoc* test. This analysis is included as Appendix 6.

Therefore, reduction of IL-6 may diminish neuroprotection while also reducing inflammation.

To confirm that the increase in synthesis of IL-1β RNA corresponded to an increase in the production and release of IL-1β, we measured the levels of the cytokine in the culture medium using ELISA. TNF-α led to an 80-fold increase in IL-1β released into the medium, and this increase was reduced 58% by cotreatment with xaliproden (Figure 4). Treatment of confluent ARPE-19 cells with TNF-α led to a loss in cell count, and this loss was prevented by simultaneous treatment with xaliproden (Appendix 3).

Treatment of ARPE-19 cells that had been allowed to form tight junctions with TNF-α led to a 55% reduction in transepithelial resistance suggesting a disruption of tight junctions. Cotreatment with xaliproden mitigated this damage, and the TEER was preserved (Figure 5), corresponding to an increase in tight junctions revealed with ZO-1 immuno-histochemistry (Figure 3). This result is consistent with an increase in the synthesis of the tight junction protein occludin in the presence of TNF-α and xaliproden (Table 2).

Elevation of protective proteins in the retina: To determine whether xaliproden would lead to an elevation of protective enzymes in the retina, we fed C57Bl/6J mice xaliproden (3 mg/kg) for 4 days. Two hours after the final dose the mice were humanely sacrificed, and their retinas dissected for analysis of RNA levels with quantitative real-time PCR (Table 3). Relative to the levels of mRNA measured in the mice treated with vehicle alone, we detected a 3.9-fold increase in the level of HO-1 and Met-1 mRNA, a 3.5-fold increase in GSTM1 expression, and a 3.8-fold increase in NqO1. The extent of the increase in the expression of these genes was greater than we had observed earlier using 8-OH-DPAT [9]. The level of catalase mRNA was elevated by 50% in the drug-treated mice, similar to the level of increase seen using 8-OH-DPAT.

Xaliproden reduces the level of CEP-modified proteins in the RPE: CEP is an oxidation product of docosahexaenoic acid-containing lipids that covalently modifies proteins in Bruch's membrane and drusen in AMD eyes [35,36]. We previously showed that CEP-adducted proteins are increased in the RPE of mice depleted for MnSOD in that cell layer [16]. To determine whether the protection of RPE-like cells in culture would translate to reduced oxidative stress RPE cells in mice, we turned to our model of retinal degeneration caused by the RPE-specific deletion of the gene for MnSOD [15]. These mice exhibit a gradual decline in ERG amplitudes
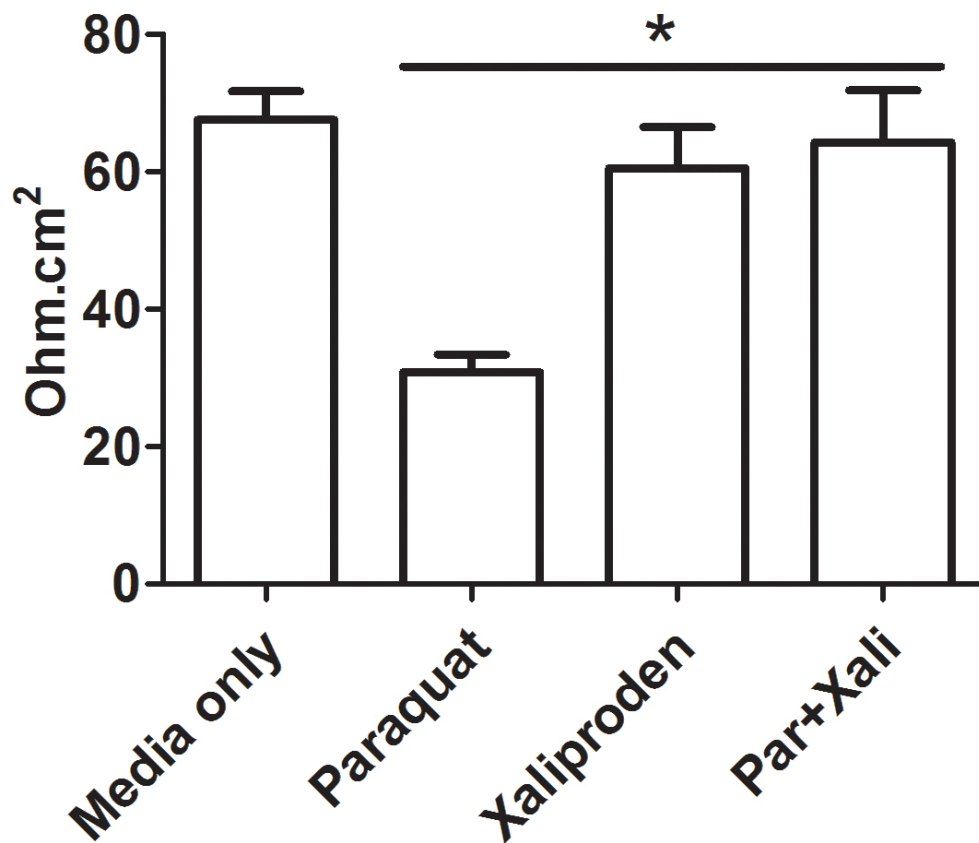

Figure 2. Xaliproden protects against the loss of tight junctions in the presence of paraquat. ARPE-19 cells were seeded in 24 Transwell plates and grown in low serum medium for 2 weeks. The cells were then treated with paraquat (300 μM), xaliproden (20 μM), or a combination of the two for 24 h before the transepithelial resistance (TEER) was measured in a volt/ohm meter. Bars represent the average electrical resistance from triplicates ± standard deviation (SD). *, p = 0.006 between paraquat, and paraquat + xaliproden, as determined with one-way ANOVA. Par = paraquat; Xali = xaliproden.

TABLE 2. XALIPRODEN EXHIBITS ANTI-INFLAMMATORY PROPERTIES.

Target gene	Relative expression ± SD.		P value
	TNFα	TNFα +Xaliproden	
IL-1β	171.3±13.8	95.2±19	0.018
IL-6	10.3±1.4	5.7±1.8	0.04
CCL-20	119.4±5.6	76.6±16	0.03
VEGFA	2.5±0.4	0.84±0.1	0.005
Occludin	1.7±0.2	2.8±1.3	0.1

ARPE-19 cells were treated with 20 μM xaliproden for 3 h, followed by treatment with TNFα (10 ng/ml) for 4 h. RNA was extracted from these cells and was used for cDNA synthesis followed by qPCR with primers for target genes indicated. Three biologic replicates were performed and expression relative to β-actin was determined. Values represent average fold change over the untreated samples ± standard deviation. P values were determined by Student *t* test for unpaired samples.
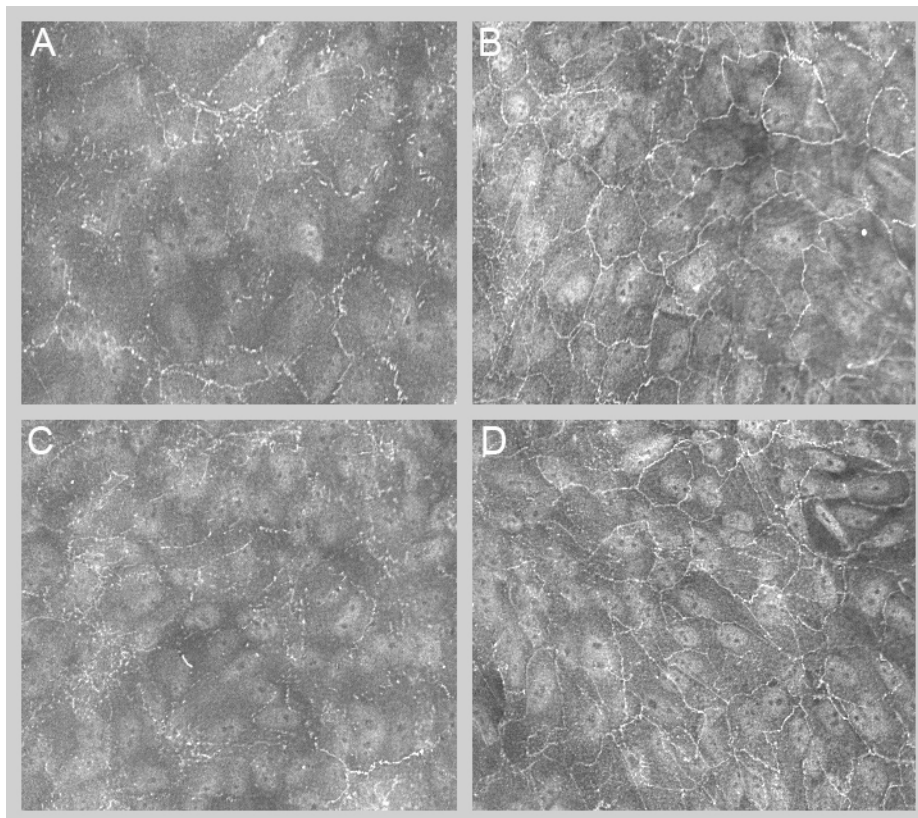

Figure 3. Xaliproden protects against the loss of tight junctions caused by oxidative stress and inflammation. ARPE-19 cells were grown for 4 weeks in low serum media until a change in the cuboidal shape was noticeable. They were then treated with 300 μM paraquat alone or in combination with xaliproden (20 μM) or left untreated for 48 h. Alternatively, the cells were treated with tumor necrosis factor-α (TNF-α; 10 ng/ml) or a combination of TNF-α and xaliproden for 48 h. Cultures were then permeabilized with 1% Triton X-100 and incubated with an antibody to zona occludens-1 (ZO-1), followed by a Cy-3 conjugated secondary antibody and viewed in a fluorescence microscope. **A**: Paraquat alone. **B**: Paraquat plus xaliproden. **C**: TNF-α alone. **D**: TNF-α plus xaliproden.
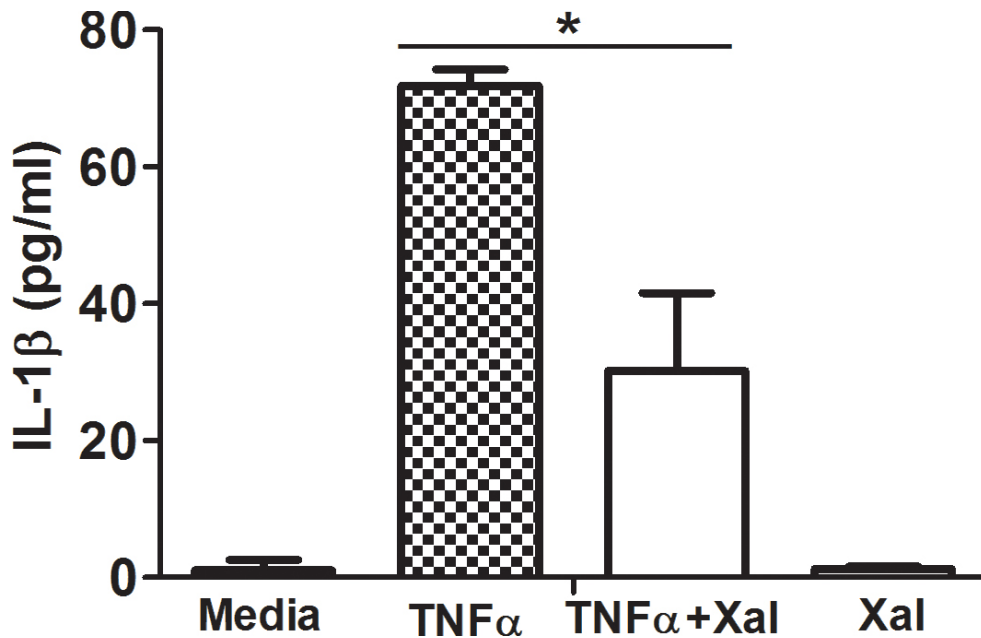
Figure 4. Xaliproden suppresses the secretion of IL-1β from cells induced with TNF-α. ARPE-19 cells were seeded at 70% confluency and grown overnight. They were incubated in serum-free media for 3 h followed by the addition of 10 ng/ml of tumor necrosis factor-α (TNF-α) or TNF-α plus 20 μM xaliproden, and the cells were grown for 15 h. Supernatants were harvested and used for quantitation of interleukin (IL)-1β in with enzyme-linked immunosorbent assay (ELISA). Bars represent the average of triplicates ± standard deviation (SD). *, p = 0.008. xal = xaliproden.

that is statistically significant only after 6 months, but they show signs of RPE and photoreceptor atrophy by 4 months. We treated the mice at two dose levels (0.5 mg/kg and 3 mg/kg) by daily gavage for 4 months starting at 1 month of age (approximately 1 week post-weaning). These levels corresponds to doses 0.04 mg/kg and 0.24 mg/kg for a 60 kg human based on body surface area [37]. The dose given in the ALS clinical trial of xaliproden was 2 mg per day, meaning that our low dose was in that range. We employed an antibody generated against CEP-conjugated human serum albumin [38] to visualize CEP-modified proteins by immunohistochemistry (Figure 6). We noted reduced staining for CEP in *Sod2*[loxP/loxP] *RPE-cre* mice treated at either level of xaliproden (0.5 or 3 mg/kg) relative to mice treated with the vehicle alone.
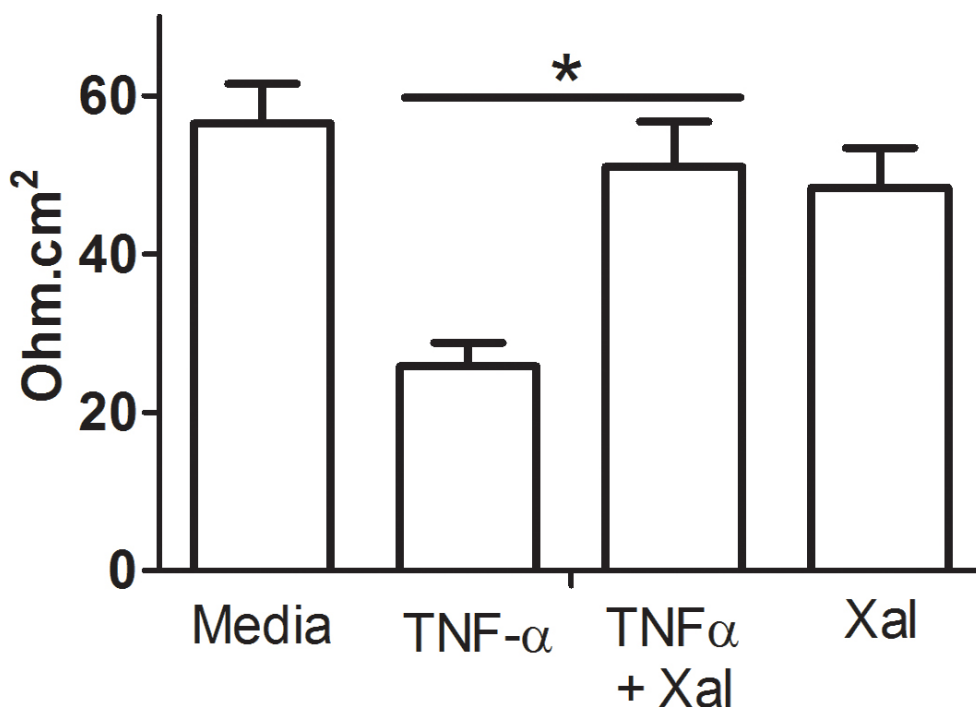

Figure 5. Xaliproden protects against the loss of tight junctions in the presence of TNF-α. ARPE-19 cells were seeded in 24 Transwell plates and grown in low serum medium for 4 weeks. The cells were then treated with tumor necrosis factor-α (TNF-α; 10 ng/ml), xaliproden (20 M), or a combination of the two or left untreated for 48 h before the transepithelial electrical resistance (TEER) was measured using a volt/ohm meter. Bars represent the average electrical resistance from triplicates ± standard deviation (SD). *, p = 0.005, as determined with one-way ANOVA. xal = xaliproden.

This result suggests that the elevation of protective proteins in response to xaliproden treatment reduces the burden of oxidized lipids in the RPE. Renganathan and colleagues had previously reported that another 5HT1a agonist, AL-8309A, reduced the level of CEP adducts in albino rats subjected to injury by blue light exposure [23].

Xaliproden improves visual function and retinal structure: We analyzed retinal function in these mice using the optokinetic response by OptoMotry™. Measuring acuity with this approach does not average the response of the full retina, as does full-field ERG, so that acuity measurements appear to be more sensitive to the impact of injury [39] or, conversely, to rescue [40] in some cases. Treatment with 0.5 mg/kg xaliproden led to a 28% improvement in visual acuity and treatment with 3 mg/kg to a 31% improvement relative to mice treated with vehicle alone (Figure 7A). This improvement in behavior performance was paralleled by a slight, but statistically significant, increase in the thickness of the outer nuclear layer in mice treated with either dose level of xaliproden, suggesting improved survival of the photoreceptor cells (Figure 7B).

Despite the relative protection of the outer nuclear layer (ONL) thickness and visual acuity afforded by xaliproden, we observed no comparable impact of the drug on ERG amplitudes. After 4 months of treatment, we observed no significant difference in a-wave and b-wave amplitudes between $Sod2^{loxP/loxP}$ *RPE-cre* mice treated with vehicle or either dose of xaliproden (Figure 8). However, as expected from our earlier characterization of this model, the ERG amplitudes were not significantly changed at this time point. There was no significant difference between the amplitudes measured at 2 months and those measured at 4 months (Figure 8 and Appendix 4). Similarly, we observed no significant difference in photopic ERG b-wave amplitudes between mice treated with vehicle alone or with the low dose of xaliproden (0.5 mg/kg), but we noticed a depression of the photopic ERG response at 4 months in mice treated at the higher dose (3 mg/kg). This reduction was statistically significant relative to the low-dose-treated mice and may reflect a harmful effect of prolonged high-dose treatment that was not apparent with SD-OCT or optokinetic measurements (Figure 7).

Xaliproden treatment preserved the structure of the RPE and photoreceptors: At the conclusion of 4 months of treatment, the eyes of mice from each treatment group were prepared for electron microscopy. Even at low magnification (Figure 9), the difference between the control-treated $Sod2^{loxP/loxP}$ *RPE-cre* mice and those treated at either dose level of xaliproden was apparent. The RPE of vehicle-treated mice was thinner and exhibited abundant vacuoles that contained membrane fragments. The increase in RPE vacuolization extended along the entire periphery of the retina as revealed with light microscopy (Appendix 5). Nuclei of the RPE cells were irregular and condensed, typical of dying cells, and the in-foldings at the basal surface of the RPE were distended. Photoreceptor outer segments were broken and contained cystic spaces. The stacking of disc membranes in the rod outer segments appeared disrupted. In contrast, the RPE of xaliproden-treated mice did not contain massive vacuoles, and the basal in-foldings appeared condensed. Photoreceptor outer segments were continuous, and disc membranes were compact and regularly stacked. At higher magnification (Figure 10), the RPE of xaliproden-treated mice exhibited more mitochondria along the basal surface and vertically displaced melanosomes typical of normal RPE, features lacking in the control mice. Treatment with the drug also reduced the accumulation of lipofuscin-containing vesicles seen in the vehicle-treated mice.

Target gene	Relative expression (versus β-actin) ± SD.		Fold induction	P value
	Saline	Xaliproden		
HO-1	2.91±0.68	11.4±3.6	3.9	0.01
GSTM-1	46.64±16	163.7±30.3	3.5	0.002
NqO-1	0.66±0.23	2.5±0.67	3.8	0.007
CAT	39.88±11.5	63.0±14	1.58	0.03
Met-1	77.45±12.3	301±34	3.88	0.007

TABLE 3. XALIPRODEN ADMINISTRATION BY ORAL GAVAGE INDUCES ANTIOXIDANT RESPONSE IN MOUSE RETINA.

Mice (C57BL/6, 4 −6 weeks old, n=5) were given xaliproden (3 mg/kg), or saline as control by oral gavage once daily for four days. On fourth day, eyes were enucleated, dissected obtain the retina. RNA was extracted and used to carry out qPCR for the antioxidant genes expression relative to β-actin. Values represent average fold change over the saline treated mice (both relative to β-actin) ± SD. Abbrev: HO-1, heme oxygenase; GSTM1, glutathione S-transferase Mu-1; NqO-1, NAD(P)H dehydrogenase Mu-1; CAT, catalase, Met-1, metallothionein-1. P values were determined using Student *t* test for unpaired samples.
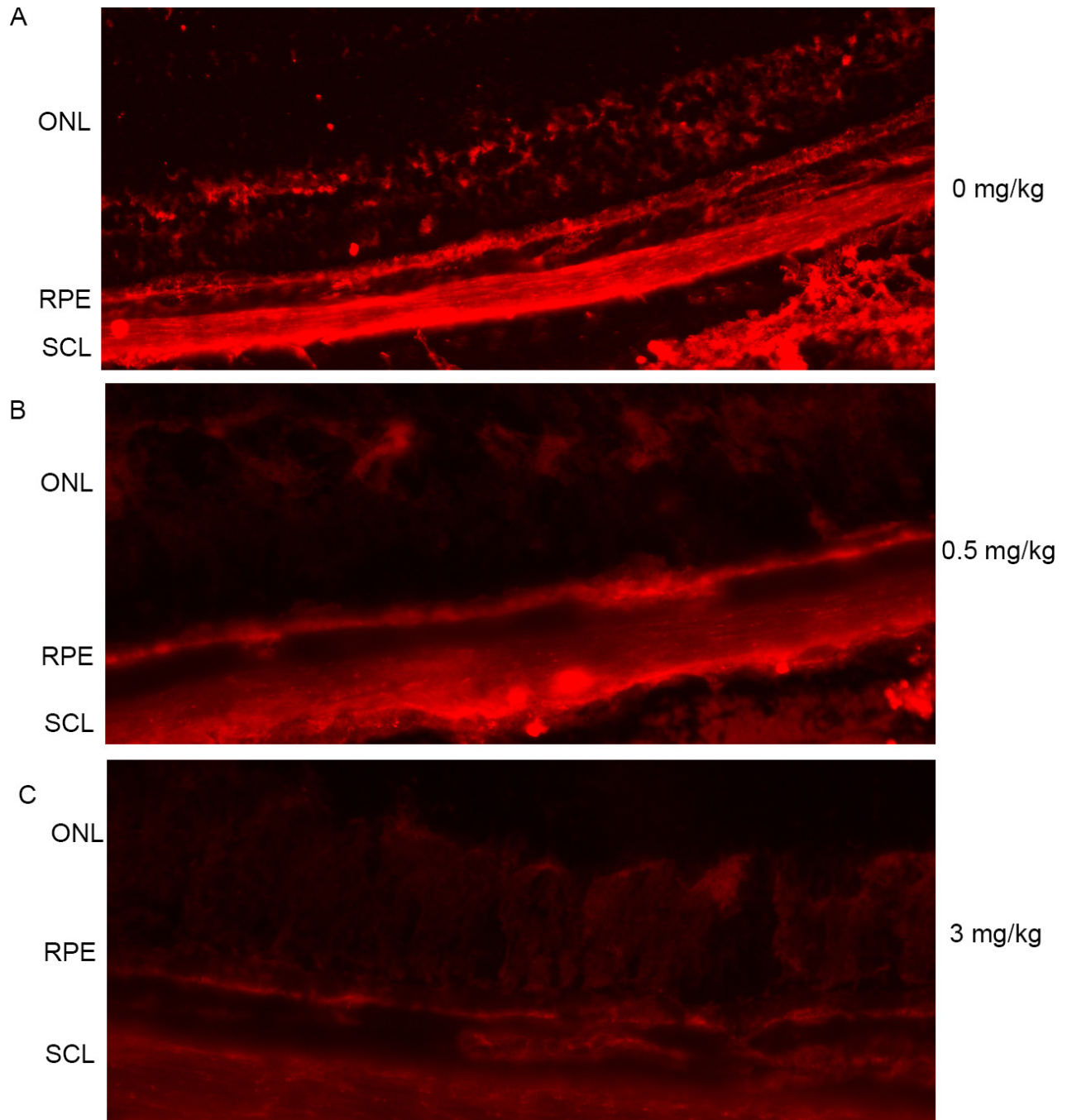
Figure 6. Decrease in CEP-modified proteins in retinal pigment epithelium (RPE) of xaliproden-treated mice. Frozen sections of eyes from *Sod2* knockout mice prepared following 4 months of oral dosing with xaliproden at (**A**) 0 mg/kg (vehicle), (**B**) 0.5 mg/kg, or (**C**) 3 mg/kg. Primary antibody was a gift of John Crabb of the Cleveland Clinic Research Foundation and was raised against carboxyethylpyrrole (CEP)-modified serum albumin outer nuclear layer (ONL); sclera (SCL). Secondary antibody was Alexa Fluor® 594 goat anti-mouse immunoglobulin G (IgG; Life Technologies, Cat No: A11005).

DISCUSSION

The induction of antioxidant (Table 1) and anti-inflammatory (Table 2) genes by xaliproden may explain the protective properties of this drug in models of peripheral neuropathy [41] and the anti-inflammatory effects of the drug in the EAE model [42]. These properties provided hope that xaliproden would be a useful therapeutic for ALS, a hope that was unfulfilled in clinical trials. Nevertheless, safe and tolerable doses of this drug were identified, and in phase III trials, the drug had a small positive effect on clinical outcome. In a clinical trial of xaliproden for peripheral neuropathy caused by chemotherapy for colon cancer, xaliproden decreased neurotoxicity by 39%. Side effects of the drug included diarrhea, dizziness, anxiety, tinnitus, and vertigo and are serotonin-related [43]. These side effects are similar to the side effects of the 5HT1a

agonists currently on the market. The fact that the compound can be taken by mouth and has an established clinical profile encouraged us to consider xaliproden for treatment of age-related macular degeneration.

We tested this compound on RPE-derived cells in culture subjected to oxidative and proinflammatory stimuli and in a mouse model of RPE and retinal atrophy based on mitochondrial oxidative stress in the RPE. RPE oxidative stress that increases with age and the resultant chronic subacute inflammation are considered important contributory factors for AMD. At 0.25 mM, paraquat actually extends the longevity of *C. elegans* grown in culture possibly with induction of Hif-1 and AMPK [44]. In ARPE-19 cells, paraquat alone induced the production of metallothionein and the Nrf2-regulated genes *NqO1* and *GSTM1*. Others have noted that
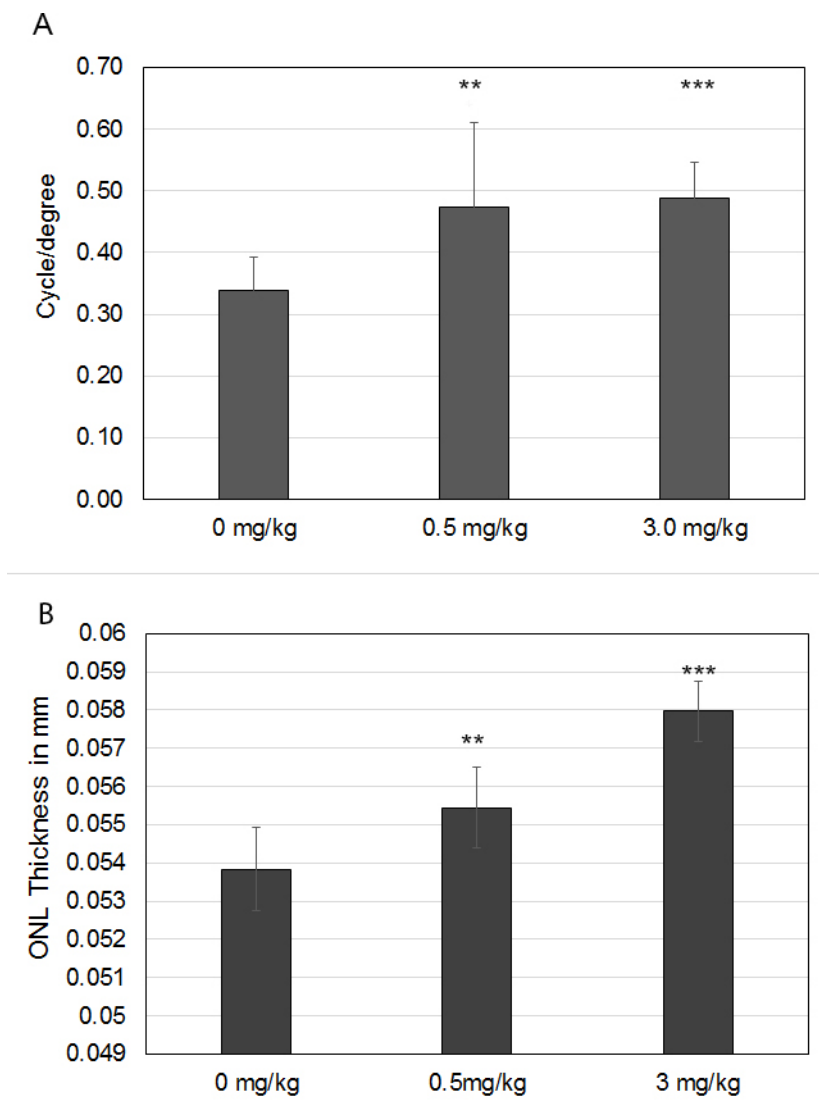

Figure 7. Xaliproden treatment leads to improved visual acuity and thicker outer nuclear layer (ONL) in *Sod2*-deleted mice. **A**: After 4 months of treatment with xaliproden at the indicated doses, the mice were assessed for visual acuity with OptoMotry™ (n = 8). **B**: After 4 months of treatment, the mice were analyzed with spectral domain optical coherence tomography (SD-OCT) for thickness of the outer nuclear layer (ONL; n = 12). **p<0.01;***p<0.001.
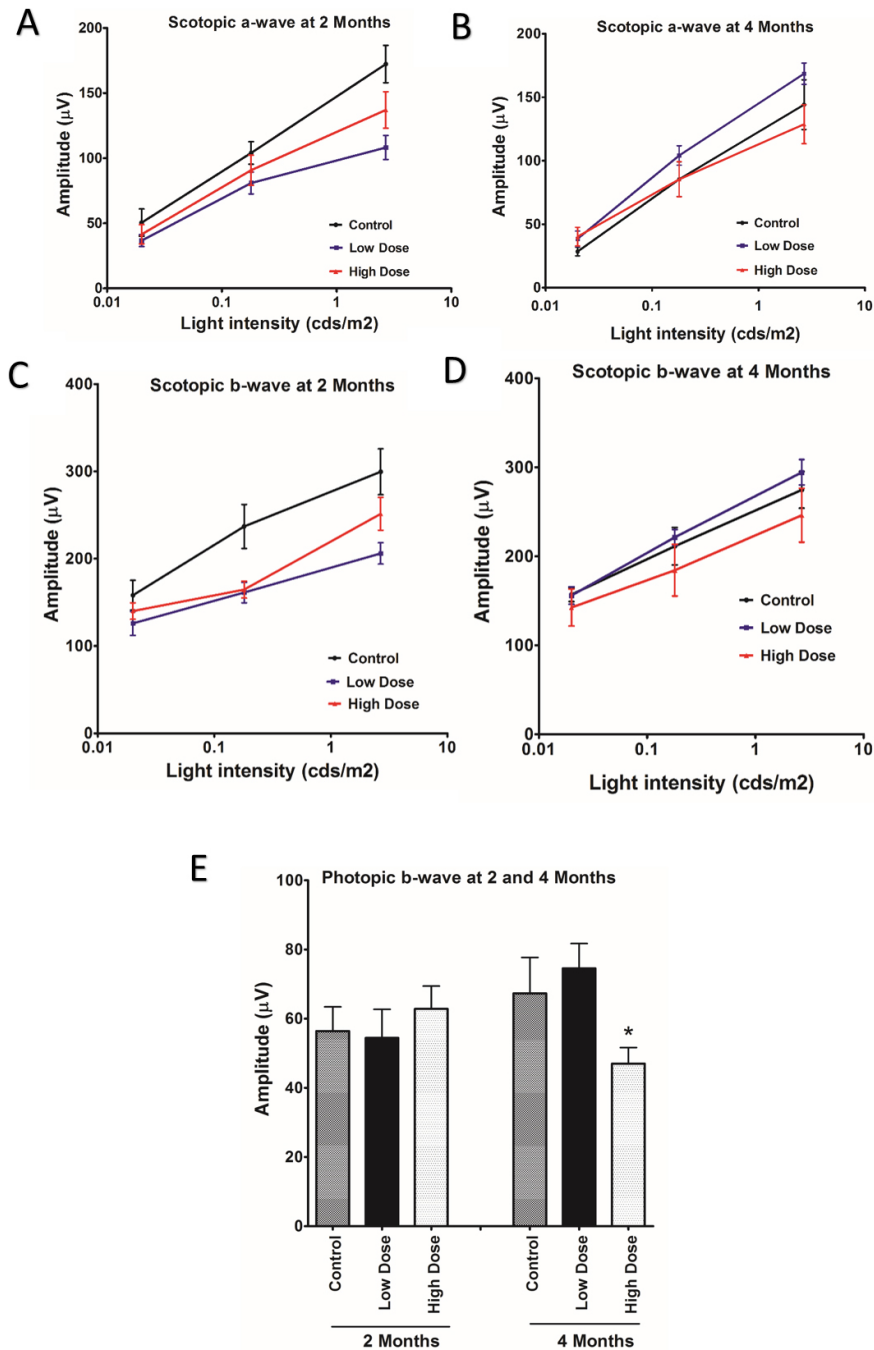
Figure 8. No difference in scotopic ERG response with drug treatment. Dark-adapted electroretinogram (ERG) amplitudes measured at three flash intensities for mice treated with 0 mg/kg (control, n = 12), 0.5 mg/kg (low dose, n = 15), or 3.0 mg/kg (high dose, n = 12) of xaliproden for 4 months. **A**: a-wave amplitudes at 2 months of treatment. **B**: a-wave amplitudes at 4 months of treatment. **C**: b-wave amplitudes at 2 months of treatment. **D**: b-wave amplitudes at 4 months of treatment. Scotopic ERGs were elicited with 1 msec flashes of white light at 0 dB (2.68 cds/m^2), −10 dB (0.18 cds/m^2), and −20 dB (0.02 cds/m^2). (n = 12). With the exception of the b-wave response at 2 weeks at the −10 dB flash intensity ($p<0.05$), we observed no statistically significant difference among the three treatment groups. **E**: Following 2 min of white light exposure, the photopic b-wave ERG amplitudes at −10 dB (0.18 cds/m^2) were measured following 2 months and 4 months of treatment with xaliproden. Control = Vehicle, low dose = 0.5 mg/kg, high dose = 3.0 mg/kg. n = 12; (*$p<0.05$, high dose versus low dose; high dose versus control not significant.) Error bars are standard error of the mean.
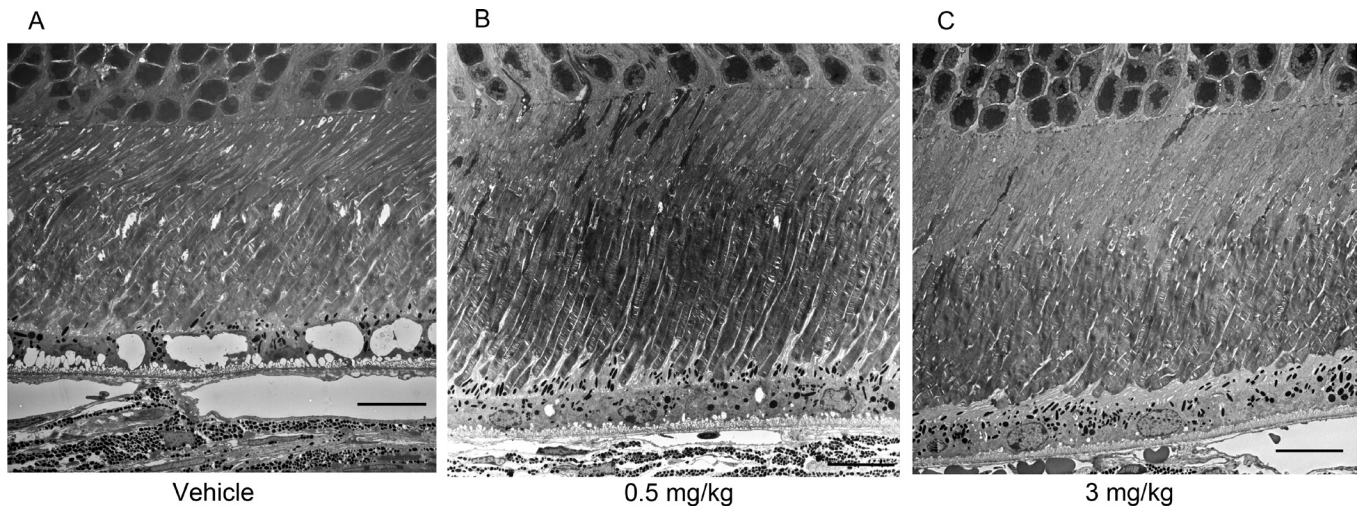
Figure 9. Damage from RPE oxidative stress is reduced by treatment with xaliproden. Electron micrographs of eyes of *Sod2*^{loxP/loxP} *RPE-cre* mice treated for 4 months with (**A**) vehicle, with (**B**) 0.5 mg/kg xaliproden, or with (**C**) 3.0 mg/kg xaliproden. Vacuoles apparent in the RPE and photoreceptor outer segments of control mice (**A**) are largely absent in the xaliproden-treated mice (**B** and **C**). Original magnification 2,000X; scale bar = 10 μm.

AMPK activation stimulates Nrf2 signaling in mammalian cells [45,46]. Nevertheless, elevation of antioxidant pathways was not sufficient to prevent the toxic effects of paraquat on ARPE-19 cells, but increased stimulation of antioxidant genes and metallothionein by the combination of paraquat and xaliproden resulted in increased survival of the same cells (Figure 1).

We have reported similar results for another 5HT1a agonist, 8-OH-DPAT [9], but in that study we did not examine the response of cultured RPE cells to proinflammatory stress. Here we report treatment of ARPE-19 cells with TNF-α led to the increased synthesis of IL-1β, IL-6, CCL20, and VEGF-A. This impact was mitigated by xaliproden (Table 2). Furthermore, TNF-α led to a breakdown of the tight junctions between RPE cells, and the integrity of the monolayer was preserved by xaliproden (Figure 5). Terasaki et al. studied the impact of TNF-α in primary porcine RPE cells and reported a difference in outcome depending on whether the cells were allowed to become polarized or not [47]. They reported that in
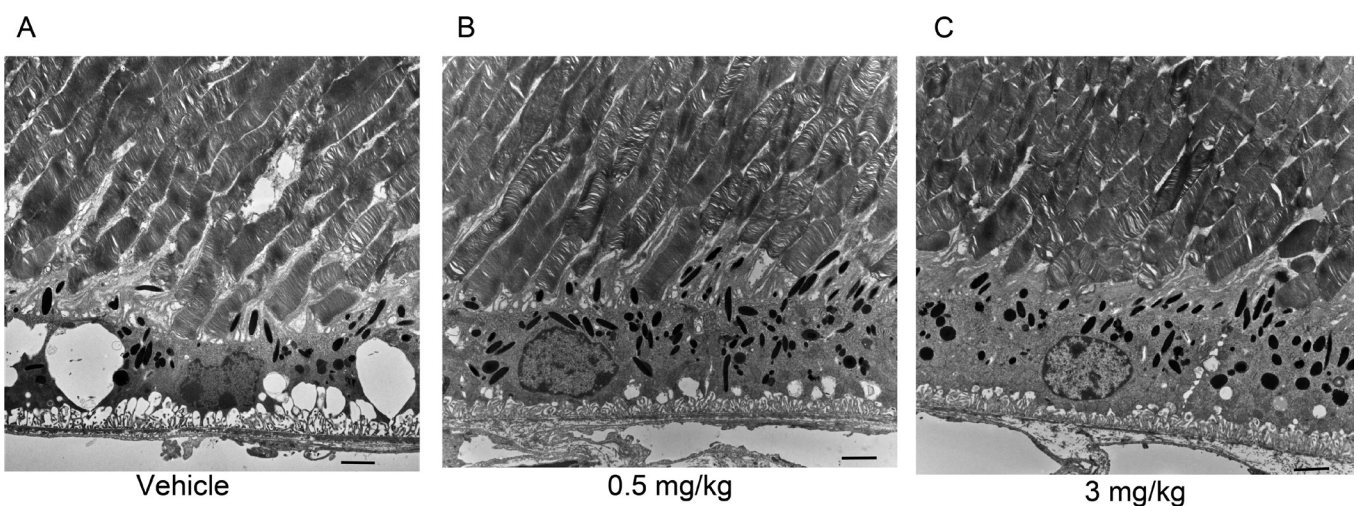

Figure 10. RPE vacuolization is mitigated by xaliproden. Electron micrographs of eyes from mice treated for of *Sod2*^{loxP/loxP} *RPE-cre* mice treated for 4 months with (**A**) vehicle, with (**B**) 0.5 mg/kg xaliproden, or with (**C**) 3.0 mg/kg xaliproden. The unfolding of the basal structure of the RPE and the large vacuoles in the RPE present in vehicle-treated eyes (**A**) is reduced in the eyes of animals fed with xaliproden. Original images 5,000X, scale bar = 2 μm.

both conditions, TNF-α stimulated the production of NF-κB p65 and that nuclear accumulation was enhanced in polarized cells. Chronic sub-acute inflammation in the RPE and retina is considered a contributory factor to the development of AMD [48], and our cell culture data suggest that xaliproden may be an effective treatment to curtail inflammatory and angiogenic signaling.

In our original description of the *Sod2*loxP/loxP *RPE-cre* mice as a model for geographic atrophy [15], we detected significant thinning of the ONL only at the 6-month time point, but we did not assess mice at 5 months, the age reported here (Figure 7B). At this age, treatment of mice with either dose level of xaliproden led to an increased thickness of the ONL relative to the control-treated mice, which we attribute to increased survival of photoreceptors. Increased thickness at this age correlated with improved visual acuity (Figure 7A) but not with improved scotopic ERG response (Figure 8). As noted above, optokinetic analysis appears to be more sensitive to small improvements in retinal function than does full-field ERG. We observed a depression in the photopic b-wave amplitude after 4 months of treatment at the high dose of xaliproden. This treatment did not correlate with damage evident by electron microscopy. Alterations in central serotonin neurotransmission can alter the implicit time of the photopic b-wave [49], and it is possible that the chronic exposure to high levels of xaliproden elicited an adaptive physiologic response that was not evident by changes in microscopic anatomy. Serotonin agonists change circadian responses to light, and chronic administration of the 5HT1a agonist buspirone caused significant changes in circadian patterns of locomotion [50]. Since photoreceptor disc shedding is governed by circadian rhythm, it is conceivable that this process was also impacted by chronic administration of a 5HT1a agonist.

Histology and electron microscopy revealed a major impact of xaliproden on the *Sod2*-deleted mice (Figure 9). A masked observer correctly differentiated treated from untreated animals based on inspection of light micrographs (Appendix 5). What distinguished eyes from untreated mice from either treatment group was the presence of numerous vacuoles in the RPE layer. Some vacuoles or separations between RPE cells were present in all of the mice, but the extent of vacuolization was far greater in the mice treated with vehicle alone. We present these results qualitatively, because accurate measurement of vacuole numbers would require serial sectioning of eyes from several mice per group, and the workforce for this effort was not available. Study of higher magnification images of the RPE revealed the normal appearance of the basal surface of the RPE in

xaliproden-treated mice, relative to the disorganized and osmophilic basal in-foldings of the vehicle-treated eyes. Similar damage to this structure has been reported in other mouse models of AMD based on inflammatory stimulation or oxidative stress [38,51-54].

Although we did not detect significant shortening of photoreceptor outer segments in the control mice (data not shown), the rod outer segments appeared broken and sometimes contained large vacuoles. Treating the mice with xaliproden prevented this photoreceptor damage. Accumulation of broken tips of photoreceptors may reflect a defect in the phagocytic function of RPE cells or in the function of RPE lysosomes in mice with unrelieved mitochondrial oxidative stress. We hope to test this hypothesis in primary RPE cultures derived from *Sod2*loxP/loxP *RPE-cre* and control mice, and to study the effects of 5HT1a agonists in this experimental system.

These data suggest that xaliproden may be an effective treatment for preventing RPE loss leading to geographic atrophy. Remaining questions concerning the use of this drug for this indication include (1) whom to treat and (2) whether the serotonergic side effects of the drug will be tolerable. We suggest that patients with mid-stage disease presenting with large irregular drusen would be candidates for treatment. Whether the side effects are acceptable depends on the dose and on the patient. One approach to avoiding side effects would be to deliver xaliproden locally instead of systemically. Recent advances in drug delivery to the back of the eye may make that route feasible [55-57].

APPENDIX 1. STR ANALYSIS.

To access the data, click or select the words "Appendix 1."

APPENDIX 2. PRIMERS FOR QPCR

To access the data, click or select the words "Appendix 2."

APPENDIX 3.

Xaliproden protects against the oxidative stress by paraquat and inflammation by TNFα. ARPE-19 cells were seeded in 8 well plates at 70% confluency and grown overnight. They were changed into serum free media and treated with paraquat (300 µM), or TNFα (10 ng/ml) alone, or in combination with xaliproden (20 µM) for 24 h, or left untreated. They were then fixed, permeabilized and stained with hematoxylin and eosin Y. Images were prepared at original magnification of 40X in a Keyence microscope. To access the data, click or select the words "Appendix 3."

APPENDIX 4. ERG WAVE FORMS

Representative ERG wave forms in dark adapted *Sod2*$^{loxP/loxP}$ *RPE-cre* mice taken after four months of treatment with 0 mg/kg (Control), 0.5 mg/kg (low dose) or 3 mg/kg (high dose) of xaliproden. Flash intensity was 2.68 cds/m^2. To access the data, click or select the words "Appendix 4."

APPENDIX 5.

Deletion of *Sod2* leads to extensive vacuolization of the RPE that is mitigated by treatment with xaliproden. **A**. Retinal hemisphere from a vehicle-treated mouse. **B**. retina from a mouse treated with 3 mg/kg of xaliproden. Plastic sections (1 μM) were stained with toluidine blue. Original magnification was 40X. Insets are electronically magnified regions from the posterior retinas. To access the data, click or select the words "Appendix 5."

APPENDIX 6. TUKEY'S MULTIPLE COMPARISON TEST OF DATA FROM TABLE 1.

X=xaliproden; p=paraquat; PX=paraquat plus xaliproden; ns=not significant; *=0.01 to 0.05; **=0.001 to 0.01; ***=0.0001 to 0.001. q=, where D is difference in means and SED is the standard error of that difference. To access the data, click or select the words "Appendix 6."

REFERENCES

1. Cowen DS. Serotonin and neuronal growth factors - a convergence of signaling pathways. J Neurochem 2007; 101:1161-71. [PMID: 17286594].

2. Saruhashi Y, Matsusue Y, Hukuda S. Effects of serotonin 1A agonist on acute spinal cord injury. Spinal Cord 2002; 40:519-23. [PMID: 12235534].

3. Bibbiani F, Oh JD, Chase TN. Serotonin 5–HT1A agonist improves motor complications in rodent and primate parkinsonian models. Neurology 2001; 57:1829-34. [PMID: 11723272].

4. Azkona G, Sagarduy A, Aristieta A, Vazquez N, Zubillaga V, Ruiz-Ortega JA, Perez-Navarro E, Ugedo L, Sanchez-Pernaute R. Buspirone anti-dyskinetic effect is correlated with temporal normalization of dysregulated striatal DRD1 signalling in L-DOPA-treated rats. Neuropharmacology 2014; 79:726-37. [PMID: 24333147].

5. Madhavan L, Freed WJ, Anantharam V, Kanthasamy AG. 5-Hydroxytryptamine 1A Receptor Activation Protects againstN-Methyl-d-aspartate-Induced Apoptotic Cell Death in Striatal and Mesencephalic Cultures. J Pharmacol Exp Ther 2003; 304:913-23. [PMID: 12604665].

6. Collier RJ, Patel Y, Martin EA, Dembinska O, Hellberg M, Krueger DS, Kapin MA, Romano C. Agonists at the serotonin receptor (5-HT(1A)) protect the retina from severe photo-oxidative stress. Invest Ophthalmol Vis Sci 2011; 52:2118-26. [PMID: 21087971].

7. Collier RJ, Wang Y, Smith SS, Martin E, Ornberg R, Rhoades K, Romano C. Complement deposition and microglial activation in the outer retina in light-induced retinopathy: inhibition by a 5–HT1A agonist. Invest Ophthalmol Vis Sci 2011; 52:8108-16. [PMID: 21467172].

8. Thampi P, Rao HV, Mitter SK, Cai J, Mao H, Li H, Lewin AS, Romano C, Boulton ME. The 5HT(1a) Receptor Agonist 8-Oh DPAT Induces Protection from Lipofuscin Accumulation and Oxidative Stress in the Retinal Pigment Epithelium. PLoS One 2012; 7:e34468-[PMID: 22509307].

9. Biswal MR, Ahmed CM, Ildefonso CJ, Han P, Li H, Jivanji H, Mao H, Lewin AS. Systemic treatment with a 5HT1a agonist induces anti-oxidant protection and preserves the retina from mitochondrial oxidative stress. Exp Eye Res 2015; 140:94-105. [PMID: 26315784].

10. Cervo L, Bendotti C, Tarizzo G, Cagnotto A, Skorupska M, Mennini T, Samanin R. Potential antidepressant properties of SR 57746A, a novel compound with selectivity and high affinity for 5–HT1A receptors. Eur J Pharmacol 1994; 253:139-47. [PMID: 8013540].

11. Martel JC. Assi+¬ MB, Bardin L, Depoort+¿re R, Cussac D, Newman-Tancredi A. 5-HT(1A) receptors are involved in the effects of xaliproden on G-protein activation, neurotransmitter release and nociception. Br J Pharmacol 2009; 158:232-42. [PMID: 19508400].

12. Appert-Collin A, Duong FH, Passilly DP, Bennasroune A, Poindron P, Warter JM, Gies JP. Xaliproden (SR57746A) induces 5–HT1A receptor-mediated MAP kinase activation in PC12 cells. Int J Immunopathol Pharmacol 2005; 18:233-44. [PMID: 15888246].

13. Meininger V, Bensimon G, Bradley WR, Brooks B, Douillet P, Eisen AA, Lacomblez L, Leigh PN, Robberecht W. Efficacy and safety of xaliproden in amyotrophic lateral sclerosis: results of two phase III trials. Amyotroph Lateral Scler Other Motor Neuron Disord 2004; 5:107-17. [PMID: 15204012].

14. Andoh T, Sakamoto A, Kuraishi Y. Effects of xaliproden, a 5-HT(1)A agonist, on mechanical allodynia caused by chemotherapeutic agents in mice. Eur J Pharmacol 2013; 721:231-6. [PMID: 24070812].

15. Mao H, Seo SJ, Biswal MR, Li H, Conners M, Nandyala A, Jones K, Le YZ, Lewin AS. Mitochondrial oxidative stress in the retinal pigment epithelium leads to localized retinal degeneration. Invest Ophthalmol Vis Sci 2014; 55:4613-27. [PMID: 24985474].

16. Justilien V, Pang JJ, Renganathan K, Zhan X, Crabb JW, Kim SR, Sparrow JR, Hauswirth WW, Lewin AS. SOD2 knockdown mouse model of early AMD. Invest Ophthalmol Vis Sci 2007; 48:4407-20. [PMID: 17898259].

17. Seo SJ, Krebs MP, Mao H, Jones K, Conners M, Lewin AS. Pathological consequences of long-term mitochondrial oxidative stress in the mouse retinal pigment epithelium. Exp Eye Res 2012; 101:60-71. [PMID: 22687918].

18. Le YZ, Zheng W, Rao PC, Zheng L, Anderson RE, Esumi N, Zack DJ, Zhu M. Inducible expression of cre recombinase in the retinal pigmented epithelium. Invest Ophthalmol Vis Sci 2008; 49:1248-53. [PMID: 18326755].

19. Strassburger M, Bloch W, Sulyok S, Schuller J, Keist AF, Schmidt A, Wenk J, Peters T, Wlaschek M, Lenart J, Krieg T, Hafner M, Kumin A, Werner S, Muller W, Scharffetter-Kochanek K. Heterozygous deficiency of manganese superoxide dismutase results in severe lipid peroxidation and spontaneous apoptosis in murine myocardium in vivo. Free Radic Biol Med 2005; 38:1458-70. [PMID: 15890620].

20. Douglas RM, Alam NM, Silver BD, McGill TJ, Tschetter WW, Prusky GT. Independent visual threshold measurements in the two eyes of freely moving rats and mice using a virtual-reality optokinetic system. Vis Neurosci 2005; 22:677-84. [PMID: 16332278].

21. Pang J, Boye SE, Lei B, Boye SL, Everhart D. Ryals, Umino Y, Rohrer B, Alexander J, Li J, Dai X, Li Q, Chang B, Barlow R, Hauswirth WW. Self-complementary AAV-mediated gene therapy restores cone function and prevents cone degeneration in two models of Rpe65 deficiency. Gene Ther 2010; 17:815-26. [PMID: 20237510].

22. Wolfrum U. Centrin- and +¦-actinin-like immunoreactivity in the ciliary rootlets of insect sensilla. Cell Tissue Res 1991; 266:231-8. .

23. Renganathan K, Gu J, Rayborn ME, Crabb JS, Salomon RG, Collier RJ, Kapin MA, Romano C, Hollyfiled JG. Crabb JW. CEP biomarkers as potential tools for monitoring therapeutics. PLoS One 2013; 8:e76325-[PMID: 24098476].

24. Castello PR, Drechsel DA, Patel M. Mitochondria Are a Major Source of Paraquat-induced Reactive Oxygen Species Production in the Brain. J Biol Chem 2007; 282:14186-93. [PMID: 17389593].

25. Nash MS, Osborne NN. Pharmacologic evidence for 5–HT1A receptors associated with human retinal pigment epithelial cells in culture. Invest Ophthalmol Vis Sci 1997; 38:510-9. [PMID: 9040484].

26. Hong GL, Liu JM, Zhao GJ, Wang L, Liang G, Wu B, Li MF, Qiu QM, Zhong Q. The reversal of paraquat-induced mitochondria-mediated apoptosis by cycloartenyl ferulate, the important role of Nrf2 pathway. Exp Cell Res 2013; 319:2845-55. [PMID: 23954820].

27. Yang W, Tiffany-Castiglioni E, Lee MY, Son IH. Paraquat induces cyclooxygenase-2 (COX-2) implicated toxicity in human neuroblastoma SH-SY5Y cells. Toxicol Lett 2010; 199:239-46. [PMID: 20851755].

28. Miao W, Hu L, Scrivens PJ, Batist G. Transcriptional regulation of NF-E2 p45-related factor (NRF2) expression by the aryl hydrocarbon receptor-xenobiotic response element signaling pathway: direct cross-talk between phase I and II drug-metabolizing enzymes. J Biol Chem 2005; 280:20340-8. [PMID: 15790560].

29. Klein R, Myers CE, Cruickshanks KJ, Gangnon RE, Danforth LG, Sivakumaran TA, Iyengar SK, Tsai MY, Klein BE. Markers of inflammation, oxidative stress, and endothelial dysfunction and the 20-year cumulative incidence of early age-related macular degeneration: the Beaver Dam Eye Study. JAMA Ophthalmol 2014; 132:446-55. [PMID: 24481424].

30. Jin M, He S, Worpel V, Ryan SJ, Hinton DR. Promotion of adhesion and migration of RPE cells to provisional extracellular matrices by TNF-alpha. Invest Ophthalmol Vis Sci 2000; 41:4324-32. [PMID: 11095634].

31. Nagineni CN, Kommineni VK, William A, Detrick B, Hooks JJ. Regulation of VEGF expression in human retinal cells by cytokines: implications for the role of inflammation in age-related macular degeneration. J Cell Physiol 2012; 227:116-26. [PMID: 21374591].

32. Ueki Y, Wang J, Chollangi S, Ash JD. STAT3 activation in photoreceptors by leukemia inhibitory factor is associated with protection from light damage. J Neurochem 2008; 105:784-96. [PMID: 18088375].

33. Leibinger M, Muller A, Gobrecht P, Diekmann H, Andreadaki A, Fischer D. Interleukin-6 contributes to CNS axon regeneration upon inflammatory stimulation. Cell Death Dis 2013; 4:e609-[PMID: 23618907].

34. Ohta K, Yamagami S, Taylor AW, Streilein JW. IL-6 Antagonizes TGF-+¦ and Abolishes Immune Privilege in Eyes with Endotoxin-Induced Uveitis. Invest Ophthalmol Vis Sci 2000; 41:2591-9. [PMID: 10937571].

35. Ebrahem Q, Renganathan K, Sears J, Vasanji A, Gu X, Lu L, Salomon RG, Crabb JW, Anand-Apte B. Carboxyethylpyrrole oxidative protein modifications stimulate neovascularization: Implications for age-related macular degeneration. Proc Natl Acad Sci USA 2006; 103:13480-4. [PMID: 16938854].

36. Gu J, Pauer GJ, Yue X, Narendra U, Sturgill GM, Bena J. Gu,X.; Peachey,N.S.; Salomon,R.G.; Hagstrom SA, Crabb JW. Proteomic and Genomic Biomarkers for Age-Related Macular Degeneration. Adv Exp Med Biol 2010; 664:411-7. [PMID: 20238042].

37. Reagan-Shaw S, Nihal M, Ahmad N. Dose translation from animal to human studies revisited. FASEB J 2008; 22:659-61. [PMID: 17942826].

38. Hollyfield JG, Bonilha VL, Rayborn ME, Yang X, Shadrach KG, Lu L, Ufret RL, Salomon RG, Perez VL. Oxidative damage-induced inflammation initiates age-related macular degeneration. Nat Med 2008; 14:194-8. [PMID: 18223656].

39. McGill TJ, Prusky GT, Douglas RM, Yasumura D, Matthes MT, Lowe RJ, Duncan JL, Yang H, Ahern K, Daniello KM, Silver B, LaVail MM. Discordant anatomical, electrophysiological, and visual behavioral profiles of retinal degeneration in rat models of retinal degenerative disease. Invest Ophthalmol Vis Sci 2012; 53:6232-44. [PMID: 22899760].

40. McGill TJ, Lund RD, Douglas RM, Wang S, Lu B, Silver BD, Secretan MR, Arthur JN, Prusky GT. Syngeneic Schwann cell transplantation preserves vision in RCS rat without immunosuppression. Invest Ophthalmol Vis Sci 2007; 48:1906-12. [PMID: 17389527].

41. Fournier J, Steinberg R, Gauthier T, Keane PE, Guzzi U. Coud+¬ FX Bougault,I.; Maffrand,J.P.; Soubri+¬,P, Le Fur G. Protective effects of SR 57746A in central and peripheral models of neurodegenerative disorders in rodents and primates. Neuroscience 1993; 55:629-41. [PMID: 8413926].

42. Bourrie B, Bribes E, Esclangon M, Garcia L, Marchand J, Thomas C, Maffrand JP, Casellas P. The neuroprotective agent SR 57746A abrogates experimental autoimmune encephalomyelitis and impairs associated bloodΓÇôbrain barrier disruption: Implications for multiple sclerosis treatment. Proc Natl Acad Sci USA 1999; 96:12855-9. [PMID: 10536012].

43. Wilkes GM, Barton-Burke M. 2015 Oncology Nursing Drug Handbook. Burlington, MA: Jones & Bartlett Publishers; 2011.

44. Hwang AB, Ryu EA, Artan M, Chang HW, Kabir MH, Nam HJ, Lee D, Yang JS. Kim,S, Mair WB, Lee C, Lee SS, Lee SJ. Feedback regulation via AMPK and HIF-1 mediates ROS-dependent longevity in Caenorhabditis elegans. Proc Natl Acad Sci USA 2014; 111:E4458-67. [PMID: 25288734].

45. Zimmermann K, Baldinger J, Mayerhofer B, Atanasov AG, Dirsch VM, Heiss EH. Activated AMPK boosts the Nrf2/HO-1 signaling axis: A role for the unfolded protein response. Free Radic Biol Med 2015; 88:417-26. [PMID: 25843659].

46. Mo C, Wang L, Zhang J, Numazawa S, Tang H, Tang X, Han XJ, Li J, Yang M, Wang Z, Wei D, Xiao H. The Crosstalk Between Nrf2 and AMPK Signal Pathways Is Important for the Anti-Inflammatory Effect of Berberine in LPS-Stimulated Macrophages and Endotoxin-Shocked Mice. Antioxid Redox Signal 2014; 20:574-88. [PMID: 23875776].

47. Terasaki H, Kase S, Shirasawa M, Otsuka H, Hisatomi T, Sonoda S, Ishida S, Ishibashi T. Sakamoto T. TNF-alpha decreases VEGF secretion in highly polarized RPE cells but increases it in non-polarized RPE cells related to crosstalk between JNK and NF-kappaB pathways. PLoS One 2013; 8:e69994-[PMID: 23922887].

48. Perez VL, Caspi RR. Immune mechanisms in inflammatory and degenerative eye disease. Trends Immunol 2015; 36:354-63. [PMID: 25981967].

49. Lavoie Jl, Illiano P, Sotnikova TD, Gainetdinov RR, Beaulieu JM. H+¬bert M. The Electroretinogram as a Biomarker of Central Dopamine and Serotonin: Potential Relevance to Psychiatric Disorders. Biol Psychiatry 2014; 75:479-86. [PMID: 23305992].

50. Smith VM, Iannatonne S, Achal S, Jeffers RT, Antle MC. The serotonergic anxiolytic buspirone attenuates circadian responses to light. Eur J Neurosci 2014; 40:3512-25. [PMID: 25195769].

51. Fujihara M, Nagai N, Sussan TE, Biswal S, Handa JT. Chronic Cigarette Smoke Causes Oxidative Damage and Apoptosis to Retinal Pigmented Epithelial Cells in Mice. PLoS One 2008; 3:e3119-[PMID: 18769672].

52. Zhao Z, Chen Y, Wang J, Sternberg P, Freeman ML, Grossniklaus HE, Cai J. Age-related retinopathy in NRF2-deficient mice. PLoS One 2011; 6:e19456-[PMID: 21559389].

53. Hu P, Herrmann R, Bednar A, Saloupis P, Dwyer MA, Yang P, Qi X, Thomas RS, Jaffe GJ, Boulton ME, McDonnell DP, Malek G. Aryl hydrocarbon receptor deficiency causes dysregulated cellular matrix metabolism and age-related macular degeneration-like pathology. Proc Natl Acad Sci USA 2013; 110:E4069-78. [PMID: 24106308].

54. Zhong Y, Li J, Wang JJ, Chen C, Tran JT, Saadi A, Yu Q, Le YZ, Mandal MN, Anderson RE, Zhang SX. X-box binding protein 1 is essential for the anti-oxidant defense and cell survival in the retinal pigment epithelium. PLoS One 2012; 7:e38616-[PMID: 22715395].

55. Rowe-Rendleman CL, Durazo SA, Kompella UB, Rittenhouse KD, Di PA, Weiner AL, Grossniklaus HE. Naash,M.I. Lewin AS, Horsager A, Edelhauser HF. Drug and gene delivery to the back of the eye: from bench to bedside. Invest Ophthalmol Vis Sci 2014; 55:2714-30. [PMID: 24777644].

56. Yamada N, Olsen TW. Routes for Drug Delivery to the Retina: Topical, Transscleral, Suprachoroidal and Intravitreal Gas Phase Delivery. Dev Ophthalmol 2016; 55:71-83. [PMID: 26501685].

57. Cholkar K, Gunda S, Earla R, Pal D, Mitra AK. Nanomicellar Topical Aqueous Drop Formulation of Rapamycin for Back-of-the-Eye Delivery. AAPS PharmSciTech 2015; 16:610-22. [PMID: 25425389].